

One Model, Two Minds: Task-Conditioned Reasoning for Unified Image Quality and Aesthetic Assessment

Wen Yin

University of Electronic Science and
Technology of China
Chengdu, Sichuan, China
Jiigan Technology
Chengdu, Sichuan, China
yinwen1999@std.uestc.edu.com

Cencen Liu

University of Electronic Science and
Technology of China
Chengdu, Sichuan, China
Jiigan Technology
Chengdu, Sichuan, China
202411900402@std.uestc.edu.com

Dingrui Liu

Bing Su
Jiigan Technology
Chengdu, Sichuan, China
liudingrui@jiigan.com
subing@jiigan.com

Yuan-Fang Li

Faculty of Information Technology,
Monash University
Melbourne, Australia
yuanfang.li@monash.edu

Tao He*

The Laboratory of Intelligent
Collaborative Computing of UESTC
Chengdu, Sichuan, China
tao.he01@hotmail.com

Abstract

Unifying Image Quality Assessment (IQA) and Image Aesthetic Assessment (IAA) in a single multimodal large language model is appealing, yet existing methods adopt a task-agnostic recipe that applies the same reasoning strategy and reward to both tasks. We show this is fundamentally misaligned: IQA relies on low-level, objective perceptual cues and benefits from concise distortion-focused reasoning, whereas IAA requires deliberative semantic judgment and is poorly served by point-wise score regression. We identify these as a *reasoning mismatch* and an *optimization mismatch*, and provide empirical evidence for both through controlled probes. Motivated by these findings, we propose TATAR (Task-Aware Thinking with Asymmetric Rewards), a unified framework that shares the visual-language backbone while conditioning post-training on each task’s nature. TATAR combines three components: fast-slow task-specific reasoning construction that pairs IQA with concise perceptual rationales and IAA with deliberative aesthetic narratives; two-stage SFT+GRPO learning that establishes task-aware behavioral priors before reward-driven refinement; and asymmetric rewards that apply Gaussian score shaping for IQA and Thurstone-style completion ranking for IAA. Extensive experiments across eight benchmarks demonstrate that TATAR consistently outperforms prior unified baselines on both tasks under in-domain and cross-domain settings, remains competitive with task-specific specialized models, and yields more stable training dynamics for aesthetic assessment.

Our results establish task-conditioned post-training as a principled paradigm for unified perceptual scoring. Our code is publicly available at <https://github.com/yinwen2019/TATAR>.

ACM Reference Format:

Wen Yin, Cencen Liu, Dingrui Liu, Bing Su, Yuan-Fang Li, and Tao He. 2026. One Model, Two Minds: Task-Conditioned Reasoning for Unified Image Quality and Aesthetic Assessment. In *Proceedings of Make sure to enter the correct conference title from your rights confirmation email (Conference acronym 'XX)*. ACM, New York, NY, USA, 10 pages. <https://doi.org/XXXXXXXX.XXXXXXX>

1 Introduction

Images are judged on two distinct axes in the real world: *technical quality* (whether blur, noise, or compression has degraded perceptual fidelity) and *aesthetic appeal* (whether composition, lighting, and semantic expressiveness combine into something visually compelling). Image Quality Assessment (IQA) [15, 46, 49, 51] and Image Aesthetic Assessment (IAA) [23, 29, 47, 52] formalize these two axes, and both are indispensable in modern visual pipelines spanning image acquisition [14], transmission [8, 33], content recommendation [13], and creative assistance [26]. In practice, users routinely expect a single system to answer both: *is this image technically good?* and *is it beautiful?* This demand has motivated a growing line of work on unified IQA-IAA modeling with Multimodal Large Language Models (MLLMs) [3, 5, 6, 54].

Existing unified methods [9, 21, 44] follow a simple recipe: they share the same backbone and optimize both IQA and IAA with the same objective, either score regression [44] or a single shared reinforcement reward [9]. This design is convenient, but it assumes the two tasks can be solved in the same way. In practice, they require different evidence and different aggregation. IQA is largely determined by low-level, relatively objective cues; accurate scoring often reduces to detecting distortions and mapping them to fidelity degradation [11, 20, 43]. In contrast, IAA is preference-sensitive and depends more on high-level semantics, composition, lighting, and overall visual impression [7, 37]. Training them with a shared thinking style and a shared reward therefore introduces a mismatch: it either encourages unnecessary deliberation for IQA or provides

*Corresponding author.

Permission to make digital or hard copies of all or part of this work for personal or classroom use is granted without fee provided that copies are not made or distributed for profit or commercial advantage and that copies bear this notice and the full citation on the first page. Copyrights for components of this work owned by others than the author(s) must be honored. Abstracting with credit is permitted. To copy otherwise, or republish, to post on servers or to redistribute to lists, requires prior specific permission and/or a fee. Request permissions from permissions@acm.org.
Conference acronym 'XX, Woodstock, NY

© 2026 Copyright held by the owner/author(s). Publication rights licensed to ACM.
ACM ISBN 978-1-4503-XXXX-X/2026/06
<https://doi.org/XXXXXXXX.XXXXXXX>

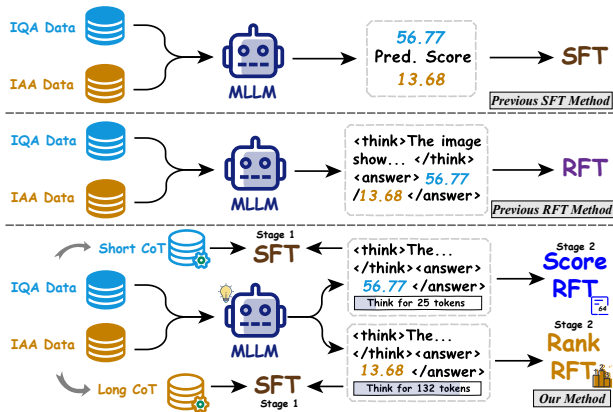


Figure 1: From shared to task-conditioned post-training. Prior unified methods apply the same response behavior and reward to both IQA and IAA, conflating two tasks with fundamentally different decision regimes. TATAR decouples *what is shared* (the VL backbone) from *what is adapted* (post-training): Stage 1 instills task-specific reasoning modes via fast–slow SFT, and Stage 2 refines scoring with asymmetric rewards matched to each task’s supervision geometry.

an overly rigid regression signal for IAA, both of which can hinder unified learning.

Building on this, a key question is raised: *in a unified IQA–IAA model, what should be shared and what should remain task-specific?* We highlight two concrete mismatches that prior unified training pipelines [9, 44] do not explicitly address: (i) **Reasoning mismatch.** IQA typically benefits from concise distortion-focused judgment: once major artifacts are identified, longer reasoning rarely improves the score and can even distract from low-level evidence. IAA, in contrast, often benefits from more deliberation to integrate multiple aesthetic factors (e.g., composition, lighting, semantics) before producing a holistic rating. A single, uniform CoT style therefore tends to be suboptimal for at least one task. (ii) **Optimization mismatch.** IQA annotations are designed to approximate an absolute fidelity scale, making point-wise score regression a natural objective. IAA annotations, however, capture subjective preference and exhibit higher ambiguity; treating them as equally precise regression targets can yield unstable optimization and poor alignment with relative human judgments.

We verify both mismatches through targeted probes. In zero-shot evaluation on KonIQ-10k [18] and ArtiMuse [10], simply prepending a chain-of-thought (CoT) instruction *improves* IAA but *degrades* IQA across four open-source MLLMs (Fig. 2a), confirming that deliberative reasoning is beneficial for one task and harmful for the other. Separately, when we train a unified model under a shared reward, IQA completions collapse to short, stable outputs while IAA completions grow longer and more variable throughout training (Fig. 2b). This divergence is not a side effect. It reveals that the two tasks occupy structurally different optimization landscapes that a single reward cannot simultaneously navigate well.

Motivated by these findings, we propose Task-Aware Thinking with Asymmetric Rewards (TATAR), a unified MLLM framework

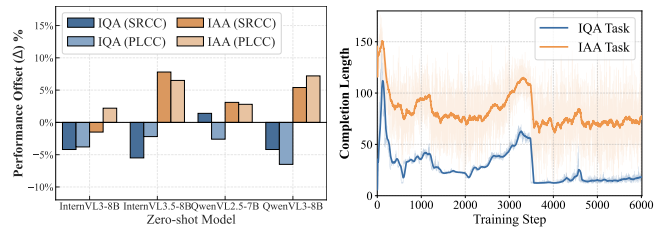


Figure 2: Motivation for task-conditioned post-training. (a) Adding a CoT instruction yields asymmetric effects: it consistently helps IAA but hurts IQA, demonstrating that a uniform reasoning strategy is suboptimal. (b) Under shared-reward RFT, IQA converges to short, stable completions while IAA produces long, variable ones, revealing that the two tasks inhabit different response and optimization regimes.

that shares a single visual–language backbone while making post-training task-aware. TATAR has three components: (i) **Fast–slow reasoning construction**, where we build task-specific rationales (QACoT–Score dataset)—concise, distortion-focused explanations for IQA (via score-conditioned reverse inference) and longer, attribute-based aesthetic rationales for IAA (via structured summarization of expert annotations); (ii) **Two-stage reasoning-mode learning**, where a format-focused supervised fine-tuning (SFT) stage stabilizes task-conditioned outputs and reasoning length, followed by GRPO [32] to refine scoring via group sampling and KL-regularized advantage optimization; and (iii) **Asymmetric reward design**, using a Gaussian score reward for IQA and a Thurstone-style completion-level ranking reward for IAA to better match their supervision characteristics and improve training stability. Critically, the asymmetry is not an ad hoc design choice. It is the direct consequence of the two mismatches diagnosed above, and our ablations confirm that swapping rewards degrades both tasks.

Extensive experiments on eight benchmarks under both in-domain and cross-domain settings show that TATAR consistently outperforms prior unified baselines, remains competitive with task-specific models, and yields more stable training dynamics for aesthetics. Our results support a broader principle that effective unified perceptual scoring requires not a one-size-fits-all objective, but *shared representation with task-conditioned adaptation*.

In summary, we make the following three contributions:

- We identify two mismatches in unified IQA–IAA: a *reasoning mismatch*, where the two tasks favor different response regimes, and an *optimization mismatch*, where a shared point-wise objective is insufficient for aesthetic judgment.
- We propose TATAR, a task-conditioned unified framework combining fast–slow reasoning construction, two-stage SFT and GRPO training, and asymmetric Gaussian score and Thurstone ranking rewards to align IQA and IAA.
- We conduct extensive experiments across 8 benchmarks, demonstrating that task-conditioned post-training is an effective and principled paradigm for unified IQA–IAA.

2 Related Work

2.1 Unified Image Quality and Aesthetic Assessment

IQA [11, 15, 20, 43, 46, 49, 51] and IAA [7, 23, 29, 37, 47, 52] have traditionally been treated as separate problems, with task-specific architectures and objectives tailored to either distortion perception or aesthetic preference. IQA focuses on perceptual fidelity under degradations such as blur, noise, and compression [18], while IAA evaluates subjective visual appeal shaped by composition, lighting, and semantics [10, 13]. The rise of MLLMs [3, 5, 6, 40, 54] has encouraged unified image scoring, where a single model handles both tasks. Existing approaches [9, 21, 44] share not only the backbone but also the training strategy, typically formulating both tasks as scalar score prediction or optimizing them under a common post-training objective. While these methods demonstrate that unified modeling is feasible, they treat IQA and IAA as homogeneous scoring problems and overlook their fundamentally different reasoning behaviors and supervision structures. Our work addresses this gap by sharing the backbone while conditioning post-training on the nature of each task.

2.2 Post-training and Reward Design for MLLMs

Post-training has become central to aligning MLLMs [12, 28, 30, 32, 34]. SFT, reinforcement learning, and preference-based optimization have all been shown to substantially improve reasoning and downstream performance in multimodal settings [4, 35, 39, 45, 48, 50, 53]. A standard practice is a two-stage pipeline where SFT first establishes the desired response format, followed by reinforcement fine-tuning to improve task performance [38, 41, 42]. Reward design is a critical factor in this pipeline. Prior work has explored score-based rewards [4, 22, 48, 53], preference optimization [41], ranking-based objectives [46], and rule-based verifiers [38, 39, 50], collectively showing that reward quality often matters as much as the choice of optimization algorithm. However, unified scoring methods typically apply a single reward across both IQA and IAA [9, 22], ignoring their different supervision geometries. Our work instead applies asymmetric rewards: a score-oriented objective for IQA and a ranking-oriented objective for IAA, each matched to the task’s underlying structure.

3 Method

Motivation. We propose TATAR, a unified framework for IQA and IAA built on a simple principle: *the representation can be shared, but the post-training should be task-conditioned*. As discussed in Sec. 1, IQA and IAA differ along two aspects. First, they favor different *reasoning regimes*: IQA is distortion-centric and benefits from concise judgments, whereas IAA often requires more deliberative aggregation of semantic and compositional cues. Second, they differ in *reward geometry*: IQA is naturally supervised by absolute quality scores, while IAA is better captured by the relative preference structure implied by aesthetic scores. TATAR addresses both mismatches within one MLLM policy.

Overview. As shown in Fig. 3&4, TATAR consists of three components. (1) **Fast–slow reasoning construction** (§3.1) builds task-specific demonstrations (QACoT–score dataset), pairing IQA with

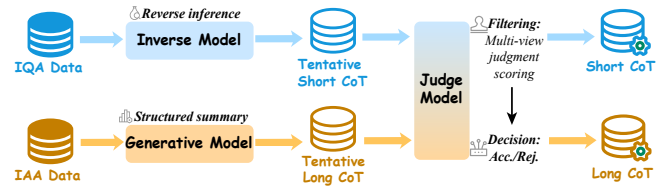


Figure 3: Task-conditioned reasoning construction. IQA rationales are synthesized by score-conditioned reverse inference from image–score pairs, while IAA rationales are obtained by summarizing structured aesthetic annotations. A unified judge then filters low-quality generations, producing the final fast–slow reasoning corpus used in Stage 1 SFT.

short perceptual rationales and IAA with longer aesthetic rationales. (2) **Task-conditioned two-stage learning** (§3.2) first uses SFT to teach the model *how* each task should be answered, then applies RFT to improve *what* score is predicted. (3) **Asymmetric reward design** (§3.3) uses score-oriented optimization for IQA and ranking-oriented optimization for IAA. Importantly, the synthesized rationales are used only to initialize task-specific response priors in Stage 1; the final model is optimized in Stage 2 by task-aligned rewards.

3.1 Fast–Slow Reasoning Construction

Existing IQA and IAA datasets provide reliable scalar scores but typically lack the task-specific reasoning traces needed to teach different response modes. We therefore construct a *fast–slow* reasoning corpus–QACoT–score dataset–that reflects the distinct decision regimes of the two tasks. The construction is task-specific, but the output format is unified: each sample contains one `<think>` field and one `<answer>` field, where `<answer>` holds the final score.

IQA: score-conditioned reverse inference. Most IQA datasets contain only an image and its mean-opinion score (MOS). To obtain concise IQA rationales, we start from such image–score pairs and prompt a strong teacher MLLM to infer a short explanation grounded in visible distortions. Concretely, using KonIQ-10k [18] as the seed dataset, the teacher is given the image and its score and asked to produce a brief rationale focused on low-level quality factors such as blur, noise, compression artifacts, exposure, and detail loss. The rationale is intentionally short and distortion-oriented, reflecting the *fast* decision regime of IQA.

IAA: structured aesthetic summarization. IAA requires a different form of supervision. We use ArtiMuse [10] as the seed dataset because it provides not only overall aesthetic scores but also rich attribute-level annotations including composition, technical execution, emotion, originality, and overall impression. Rather than inferring a rationale solely from the final score, we prompt a strong teacher model to summarize these structured attributes into a coherent long-form explanation and output the corresponding score. The goal is not to restate the annotations verbatim, but to organize them into a connected judgment process that reflects the more deliberative nature of aesthetic assessment.

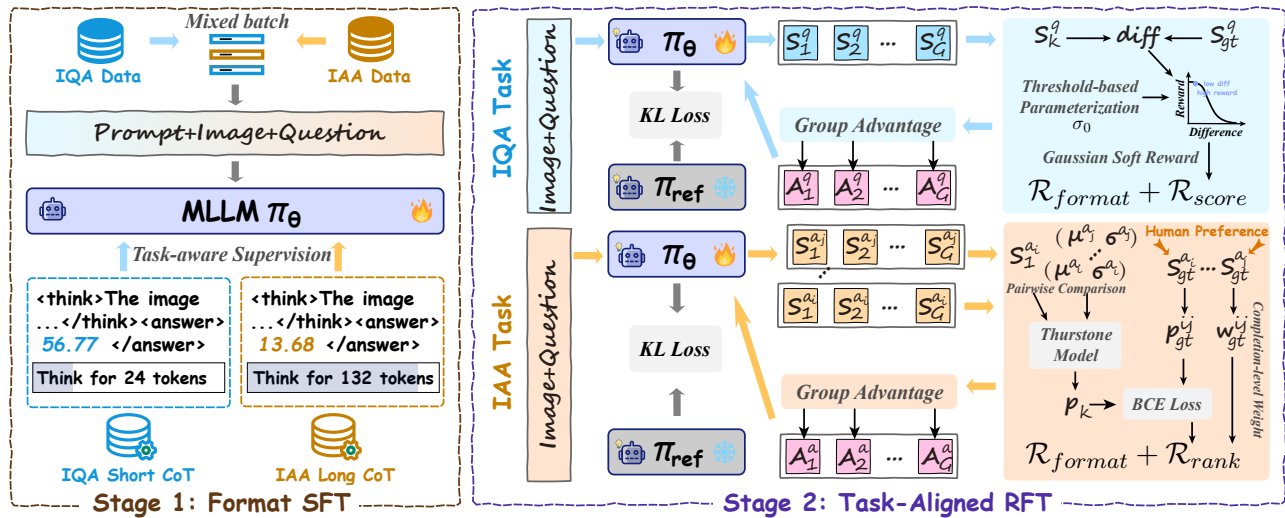


Figure 4: Overview of TATAR. TATAR is a unified framework for IQA and IAA with task-conditioned reasoning and reward design. In Stage 1, format-oriented SFT aligns the model to a shared `<think>/<answer>` output schema while teaching distinct response modes, with concise reasoning for IQA and more deliberative reasoning for IAA. In Stage 2, task-conditioned GRPO further refines the model with a shared optimization procedure but asymmetric rewards, where IQA is optimized with a Gaussian score reward $\mathcal{R}_{fmt} + \mathcal{R}_{score}$ and IAA is optimized with a ranking reward $\mathcal{R}_{fmt} + \mathcal{R}_{rank}$.

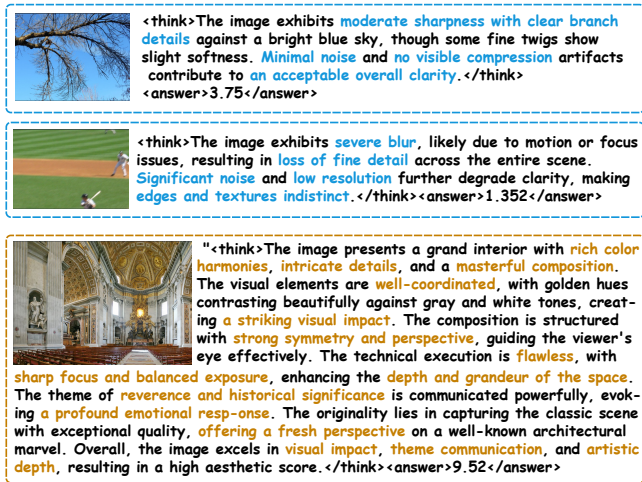


Figure 5: Two examples from the constructed reasoning corpus (QACoT-score dataset). IQA (top) samples use concise, distortion-focused rationales, while IAA (bottom) samples use longer and more integrative aesthetic rationales.

Unified judge-based filtering. Synthetic rationales are inevitably noisy, so we apply a judge-based filtering step before training. A strong judge MLLM examines each generated sample and returns an accept or reject decision. The judge first applies shared hard constraints covering output format, score validity, and general reasoning cleanliness, and then performs task-specific checks. For IQA, it verifies whether the rationale is visually grounded and whether the identified distortions are plausible. For IAA, it checks whether

the explanation covers relevant aesthetic factors, remains semantically coherent, and avoids unsupported conclusions. Only accepted samples are retained, yielding a clean task-aware reasoning corpus for Stage 1 training. Representative examples are shown in Fig. 5.

3.2 Task-Conditioned Two-Stage Learning

The constructed reasoning corpus specifies *how* the model should respond to each task, but does not by itself guarantee optimal scoring behavior. We therefore train TATAR in two stages: a supervised stage that establishes task-specific response priors, followed by a reinforcement stage that improves prediction quality under task-aligned rewards.

Stage 1: SFT for response-mode alignment. In the first stage, we fine-tune a shared policy π_θ on mixed IQA and IAA batches under a unified Prompt+Image+Question interface. All outputs are normalized to the same schema,

`<think> ... </think><answer> score </answer>`.

The key difference lies in the supervision inside `<think>`, where IQA demonstrations encourage short, perceptual rationales and IAA demonstrations encourage longer, more integrative reasoning. This stage teaches the model to adopt a task-appropriate response mode alongside predicting a score. In other words, Stage 1 establishes a behavioral prior for fast IQA reasoning and slow IAA reasoning, preventing the mode collapse observed under RL-only training (Fig. 2b).

Stage 2: GRPO for task-conditioned refinement. Starting from the SFT-initialized policy, we further optimize the model using Group Relative Policy Optimization (GRPO) [32]. For input $x = (I, q)$ consisting of an image and a task instruction, we sample a

group of G completions $\{y_k\}_{k=1}^G$ from the current policy and evaluate each with an external reward function $\mathcal{R}_k = \mathcal{R}(x, y_k)$. Rewards are normalized within the group to obtain relative advantages,

$$A_k = \frac{\mathcal{R}_k - \text{mean}(\{\mathcal{R}_1, \dots, \mathcal{R}_G\})}{\text{std}(\{\mathcal{R}_1, \dots, \mathcal{R}_G\}) + \epsilon}, \quad (1)$$

where ϵ is a small constant for numerical stability. GRPO then updates the policy to increase the likelihood of high-advantage completions while regularizing toward a frozen reference model π_{ref} initialized from Stage 1,

$$\mathcal{J}_{\text{GRPO}}(\theta) = \mathbb{E}_{x \sim \mathcal{D}, y_k \sim \pi_{\theta_{\text{old}}}} \left[\frac{1}{G} \sum_{k=1}^G \min \left(\rho_k(\theta) A_k, \text{clip}(\rho_k(\theta), 1-\xi, 1+\xi) A_k \right) - \beta D_{\text{KL}}(\pi_{\theta} \parallel \pi_{\text{ref}}) \right], \quad (2)$$

where $\rho_k(\theta) = \pi_{\theta}(y_k | x) / \pi_{\theta_{\text{old}}}(y_k | x)$. This formulation has two advantages in our setting. First, it directly optimizes end-task behavior without requiring a separate value model. Second, because Stage 1 has already established a valid response format, Stage 2 can focus on improving scoring quality rather than rediscovering output structure. The only component that differs across IQA and IAA in Stage 2 is the reward function, described next.

3.3 Asymmetric Reward Design

The optimizer is shared across tasks, but the reward should reflect the structure of each task. IQA is an absolute scoring problem where the goal is to predict a value close to the target MOS. IAA is less well modeled as strict point-wise regression, since multiple plausible aesthetic explanations may correspond to similar scores. We therefore use a shared format reward for both tasks and combine it with a task-specific reward matched to each supervision regime.

Shared format reward. For both IQA and IAA, we use a binary format reward $\mathcal{R}_{\text{fmt}} \in \{0, 1\}$ that equals 1 only when the completion contains exactly one pair of <think> and <answer> tags with a valid numeric score in the allowed range. This shared constraint discourages malformed outputs and ensures that task-specific rewards operate on comparable responses.

IQA reward: Gaussian score shaping. For IQA, the supervision is naturally score-based. Let S_k^q be the predicted score of completion k and S_{gt}^q the ground-truth MOS, with prediction error $\Delta_k^q = S_k^q - S_{\text{gt}}^q$. Instead of a hard threshold, we use a smooth Gaussian reward,

$$\mathcal{R}_{\text{score}} = \exp\left(-\frac{(\Delta_k^q)^2}{2\sigma(\Delta_k^q)^2}\right), \quad (3)$$

where the scale is mildly adaptive, $\sigma(\Delta_k^q) = \sigma_0(1 + \alpha|\Delta_k^q|/100)$. The base scale σ_0 is parameterized by an interpretable tolerance threshold τ : if an absolute error of τ should receive reward η , then $\sigma_0 = \tau / \sqrt{-2 \ln \eta}$. This design provides dense feedback near the target score while avoiding overly brittle optimization early in training. The final IQA reward is

$$\mathcal{R}_{\text{IQA}} = \mathcal{R}_{\text{fmt}} + \mathcal{R}_{\text{score}}. \quad (4)$$

IAA reward: score-induced relative ranking. For IAA, we do not assume access to explicit pairwise preference annotations. Instead, we derive a soft relative preference from scalar aesthetic scores and

optimize the model to preserve that relative structure. Consider IAA sample i and completion k predicting score $S_{k,i}^a$. Let μ_i^a and $(\sigma_i^a)^2$ denote the mean and variance of predicted scores across the sampled completions of sample i . For another IAA sample j , the soft ground-truth preference is defined as

$$p_{\text{gt}}^{ij} = \sigma\left(\frac{S_{\text{gt},i}^a - S_{\text{gt},j}^a}{\tau_a}\right), \quad (5)$$

where $\sigma(\cdot)$ is the sigmoid function and τ_a controls the softness of the target. The predicted preference for completion k of sample i against sample j follows a Thurstone-style comparison,

$$\hat{p}_k^{ij} = \sigma\left(\frac{S_{k,i}^a - \mu_j^a}{\sqrt{(\sigma_i^a)^2 + (\sigma_j^a)^2 + \delta}}\right), \quad (6)$$

where δ is a small constant for numerical stability. Since pairs with very different ground-truth scores are easy and less informative, we upweight ambiguous pairs via

$$w^{ij} = \exp\left(-\frac{|S_{\text{gt},i}^a - S_{\text{gt},j}^a|}{m}\right), \quad (7)$$

where m is a temperature parameter. The ranking loss for completion k of sample i is then

$$\mathcal{L}_{\text{rank}}^{k,i} = \frac{\sum_{j \neq i} w^{ij} \text{BCE}(p_{\text{gt}}^{ij}, \hat{p}_k^{ij})}{\sum_{j \neq i} w^{ij}}, \quad (8)$$

which is converted to a reward by normalization, $\mathcal{R}_{\text{rank}} = 1 - \mathcal{L}_{\text{rank}}^{k,i} / C_{\text{rank}}$, where C_{rank} is a normalization constant used to scale the ranking reward. The total IAA reward is

$$\mathcal{R}_{\text{IAA}} = \mathcal{R}_{\text{fmt}} + \mathcal{R}_{\text{rank}}. \quad (9)$$

Discussion. TATAR can be viewed as a unified model with task-conditioned post-training. The backbone, prompt interface, and optimization algorithm are shared, but the model is taught to respond differently and rewarded differently depending on whether the task is IQA or IAA. This design directly targets the two mismatches identified in Sec. 1: reasoning mode is aligned via fast–slow SFT, and optimization signal is aligned via asymmetric rewards. Ablation in Sec. 4.3 confirms that each contributes independently.

4 Experiments

4.1 Experimental Setup

Datasets and Metrics. We train on the KonIQ-10k training split (~7,000 images) and the ArtiMuse-10K training set (8,998 images), following [49, 52]. After applying the CoT generation and judge-based filtering pipeline described in Sec. 3.1, we retain 6,189 IQA samples and 7,726 IAA samples, forming the QACoT-Score dataset. For evaluation, we use KonIQ-10k [18] and ArtiMuse-10K [10] as in-domain benchmarks, and SPAQ [14], KADID-10k [24], and PIPAL [19] for out-of-domain IQA, and AVA [27], TAD66K [16], and Flickr-AES [31] for out-of-domain IAA. All MOS labels are linearly normalized to a unified 1–100 scale. We report Spearman Rank-order Correlation Coefficient (SRCC) and Pearson Linear Correlation Coefficient (PLCC) throughout, following [9, 44, 49].

Table 1: Performance comparison on unified IAA and IQA scoring. Results are reported as SRCC/PLCC (%). For specialized models, red columns denote in-domain and green columns denote out-of-domain evaluation. ♣ marks results cited from UniPercept [9], ♠ denotes single-task evaluation, and * denotes models retrained under our protocol.

Models	IAA task					IQA task				
	ArtiMuse-10K	AVA	TAD66K	FLICKR-AES	Avg.	KonIQ-10K	SPAQ	KADID	PIPAL	Avg.
<i>Proprietary Models</i>	<i>Large-scale pretraining, cross-domain testing</i>									
GPT-4o [1]	33.3/27.6	50.9/48.5	27.8/28.2	60.5/59.7	43.1/41.0	69.5/74.4	87.4/88.1	67.7/64.6	32.5/34.9	64.3/65.5
Llama-4 [2]	20.4/14.7	34.5/32.9	23.6/21.0	54.8/50.6	33.3/29.8	50.3/65.3	-4.1/0.7	-9.9/-0.4	-0.7/2.3	8.9/17.0
Gemini-2.5-Pro [36]	18.7/3.5	24.8/10.0	14.3/3.7	35.7/20.6	23.4/9.5	58.2/31.6	8.7/21.2	43.6/27.4	22.5/-1.9	33.3/19.6
Claude-4.5 [25]	4.1/2.7	0.3/1.3	4.0/4.7	3.7/4.9	3.0/3.4	-3.7/-4.3	3.6/8.5	22.3/27.3	-13.1/-8.8	2.3/5.7
<i>Open-Source Models</i>	<i>Large-scale pretraining, cross-domain testing</i>									
LLaVA-1.5-8B [3]	27.4/21.2	38.1/37.8	21.3/22.4	58.6/54.1	36.4/33.9	63.9/74.4	-/-	50.5/53.4	41.7/40.7	52.0/56.2
GLM-4.5 [17]	34.6/24.9	46.4/42.0	28.9/27.8	65.1/59.7	43.8/38.6	72.1/76.5	-4.0/-3.8	-14.2/-12.8	1.3/2.0	13.8/15.5
InternVL3-78B [54]	22.3/20.6	38.5/34.4	22.1/22.0	51.8/43.3	33.7/30.1	63.5/67.6	84.9/85.2	57.9/55.3	41.5/45.7	61.9/63.4
InternVL3.5-38B [40]	21.9/17.5	35.9/35.7	20.1/20.8	55.9/52.9	33.4/31.7	57.8/65.2	84.0/83.1	56.8/53.7	44.8/45.7	60.8/61.9
QwenVL-2.5-72B [6]	23.3/19.7	40.8/38.7	23.2/23.5	62.6/58.9	37.5/35.2	76.2/82.0	-/-	60.6/57.0	38.1/40.7	58.3/59.9
QwenVL-3-32B [5]	22.7/13.0	35.3/19.8	20.0/9.5	57.2/41.3	33.8/20.9	79.6/83.8	69.0/65.7	67.3/68.2	41.4/40.2	64.3/64.4
<i>Specialized Models</i>	<i>In-domain</i>	<i>Cross-domain</i>			<i>Avg.</i>	<i>In-domain</i>	<i>Cross-domain</i>			<i>Avg.</i>
ArtiMuse♣ [10]	61.4/62.7	39.7/38.5	23.0/23.2	34.9/33.4	39.8/39.5	-/-	-/-	-/-	-/-	-/-
DeQA♣ [49]	-/-	-/-	-/-	-/-	-/-	95.3/94.1	89.5/89.6	69.4/68.7	47.2/47.8	75.3/75.0
Q-Align♣ [44]	55.1/57.3	39.8/38.6	19.4/19.7	13.7/12.3	32.0/32.0	94.1/94.0	88.6/88.7	67.4/68.4	40.3/41.9	72.6/73.3
Q-Insight♣ [22]	-/-	-/-	-/-	-/-	-/-	93.3/91.6	90.7/90.5	74.2/73.6	48.6/47.4	76.7/75.8
Q-Insight♣ [22]	22.8/17.5	40.5/37.6	21.2/21.7	61.7/53.7	36.6/32.6	73.3/75.0	80.0/93.8	58.0/54.8	36.9/36.8	62.1/65.1
UniPercept* [9]	43.2/45.1	53.5/50.9	30.6/31.2	52.1/53.4	44.8/45.1	90.1/92.2	83.0/82.6	68.2/68.5	45.9/46.8	71.8/72.5
TATAR (Ours)	58.6/59.5	51.8/52.4	33.4/34.9	60.4/63.3	51.0/52.5	94.1/94.2	89.7/89.4	73.1/72.7	50.1/49.8	76.7/76.5

Evaluated Models. We compare against 19 models across four categories. (1) *Proprietary MLLMs*: GPT-4o [1], Llama-4-Scout [2], Gemini-2.5-Pro [36], Claude-Sonnet-4.5 [25], and Claude-Sonnet-4.5-Think [25]. (2) *Open-source MLLMs*: InternVL3 and InternVL3.5 series [40, 54], QwenVL-2.5 and QwenVL-3 series [5, 6], GLM-4.5V [17], and LLaVA-1.5 [3]. (3) *Specialized models*: Q-Align [44], ArtiMuse [10], DeQA [49], and Q-Insight [22]. (4) *Unified scoring*: UniPercept [9], retrained under the same data and protocol as ours for a fair comparison.

Implementation Details. We adopt Qwen-2.5-VL-7B-Instruct [6] as the base model for all experiments. For GRPO, we set the number of sampled generations per input to $N = 8$, the KL penalty weight to $\beta = 10^{-3}$. We use AdamW with an initial learning rate of 10^{-6} , linearly decayed to 10^{-9} . Stage 1 (Format SFT) is trained for 1 epoch, followed by Stage 2 RFT for 2–3 epochs, with a total batch size of $8 \times 2 \times 8$ on 8 NVIDIA A800 GPUs. For heterogeneous image resolutions across IQA/IAA datasets, we cap the maximum number of image pixels to 1,572,864 pixels. For the Gaussian score reward, we set $\alpha_{\text{IQA}} = 0.8$, $\alpha_{\text{IAA}} = 2.0$ (If used in Ablation), the target level $\eta = 0.5$, and the difference threshold τ to 8.75. For the ranking reward, the soft preference temperature τ is set to 0.08, and the hard-pair weighting temperature m is set to 0.12.

4.2 Main Results

Tab. 1 reports SRCC/PLCC on all eight benchmarks. TATAR achieves the best average performance on both tasks, with an IAA average of 51.0/52.5 and an IQA average of 76.7/76.5. Compared with the unified baseline UniPercept, TATAR improves IAA by +6.2/+7.4 points

and IQA by +4.9/+4.0 points, demonstrating that task-conditioned post-training consistently outperforms a shared optimization recipe across both tasks and all evaluation settings.

Comparison with proprietary models. Among proprietary models, GPT-4o achieves the most competitive results, with an IAA average of 43.1/41.0 and an IQA average of 64.3/65.5, but still falls short of TATAR by 7.9/11.5 points on IAA and 12.4/11.0 points on IQA, despite having no training on the evaluation domains. Gemini-2.5-Pro, Llama-4-Scout, and Claude-Sonnet-4.5 show substantially degraded performance, with several benchmarks yielding near-zero or negative SRCC. We attribute this to score-range misalignment: these models tend to output scores concentrated in a narrow band that does not align with the annotation scale, leading to low correlation regardless of underlying capability. This is a prompt-induced failure mode rather than a fundamental limitation, but it highlights the sensitivity of zero-shot scoring to output calibration.

Comparison with open-source models. Open-source MLLMs show a clear task asymmetry: models such as QwenVL-3-32B achieve competitive IQA performance (79.6/83.8 in-domain) but weak IAA performance (33.8/20.9 average), consistent with the observation that aesthetic judgment requires higher-level semantic integration that general-purpose pretraining does not reliably provide. GLM-4.5 shows the opposite pattern on IQA: strong in-domain performance (72.1/76.5) but severe degradation on out-of-domain benchmarks including negative SRCC on KADID (-14.2/-12.8), suggesting poor cross-domain generalization. TATAR improves over all open-source models on both tasks and generalizes substantially better across domains, with a +7.2/+8.3 IQA average gain over the strongest open-source model QwenVL-3-32B.

Table 2: Ablation study on training paradigm and reward design. Results are reported as SRCC/PLCC (%). Bold and underlined values indicate first and second place. Task-cond. means Gaussian for IQA and Rank for IAA.

Settings			IAA task					IQA task				
SFT	RL	Reward	ArtiMuse	AVA	TAD66K	FLICKR	Avg.	KonIQ	SPAQ	KADID	PIPAL	Avg.
✓			45.9/45.1	30.3/34.2	18.9/19.7	36.3/37.8	32.9/34.2	89.2/91.8	81.5/82.3	70.9/69.0	40.2/41.2	70.5/71.1
	✓	Hard-only	40.0/43.1	56.1/55.1	30.5/31.3	53.4/53.4	45.0/45.7	90.1/92.2	82.1/81.7	70.3/68.5	41.3/41.5	70.9/71.0
	✓	Gauss.-only	40.8/43.7	52.1/52.3	31.2/31.9	54.0/54.1	44.5/45.5	90.8/92.6	82.6/82.1	69.9/68.2	42.0/42.1	71.3/71.2
	✓	Rank-only	41.3/44.1	<u>55.8/51.4</u>	30.9/31.6	54.6/54.8	45.6/45.5	91.2/92.9	82.3/81.9	70.8/69.1	42.6/42.8	71.7/71.7
	✓	Task-cond.	41.7/44.6	55.6/51.3	31.3/32.0	55.0/55.2	46.0/45.9	91.7/93.2	82.8/82.3	71.3/69.6	43.0/43.2	72.2/72.1
✓	✓	Hard-only	55.5/53.8	46.6/43.5	30.0/29.8	56.6/52.4	47.2/44.9	90.1/91.4	84.0/85.6	71.7/66.6	43.1/43.5	72.2/71.8
✓	✓	Gauss.-only	56.6/57.5	47.9/49.1	30.2/32.7	58.4/59.7	49.7/50.7	92.5/93.6	88.2/87.9	<u>73.2/70.0</u>	45.9/47.2	75.0/74.7
✓	✓	Rank-only	<u>57.8/58.6</u>	<u>50.3/50.9</u>	<u>31.8/33.9</u>	<u>59.2/61.0</u>	<u>50.3/51.6</u>	<u>93.3/93.9</u>	<u>88.9/88.6</u>	73.0/71.5	<u>47.8/48.3</u>	<u>75.4/75.6</u>
✓	✓	Task-cond.	58.6/59.5	51.8/52.4	33.4/34.9	60.4/63.3	51.0/52.5	94.1/94.2	89.7/89.4	73.1/72.7	50.1/49.8	76.7/76.5

Comparison with specialized models. On IQA, TATAR matches the in-domain performance of the best specialized model DeQA (94.1/94.2 vs. 95.3/94.1) while simultaneously handling IAA, which DeQA cannot. On out-of-domain IQA, TATAR outperforms DeQA on SPAQ (89.7/89.4 vs. 89.5/89.6), KADID (73.1/72.7 vs. 69.4/68.7), and PIPAL (50.1/49.8 vs. 47.2/47.8). On IAA, TATAR substantially surpasses the specialized ArtiMuse model on cross-domain benchmarks (51.0/52.5 unified average vs. 39.8/39.5), with particularly strong gains on Flickr-AES (60.4/63.3 vs. 34.9/33.4) and ArtiMuse in-domain (58.6/59.5 vs. 61.4/62.7, competitive despite being a unified model). These results confirm that task-conditioned unification does not sacrifice task-specific accuracy for breadth.

4.3 Ablation Studies

Effect of training paradigm. We compare three configurations: SFT only, RL only, and the full two-stage SFT+RL. SFT alone yields a weak IAA average of 32.9/34.2, far below any RL-based configuration. This is expected: supervised imitation on the reasoning corpus teaches response format but cannot directly align the scoring policy with the target metrics. RL-only training recovers substantially, reaching IAA averages of 44.5–46.0/45.5–45.9 across reward variants, but at the cost of output instability: completion lengths collapse and format rewards stay low (Fig. 6b), indicating the model degenerates toward short, reward-seeking responses without SFT’s structural prior. On IQA, RL-only achieves 70.9–72.2/71.0–72.1, which is already competitive but still consistently below the best two-stage configurations. Combining SFT with RL yields the strongest overall performance, with the full configuration reaching 51.0/52.5 on IAA and 76.7/76.5 on IQA. Compared with the best RL-only variant, this corresponds to gains of +5.0/+6.6 on IAA and +4.5/+4.4 on IQA. These results confirm that SFT and RL are complementary: SFT establishes a stable behavioral prior, which RL then refines toward task-aligned scoring.

Effect of reward design. We compare four reward configurations: Hard-only, Gauss.-only, Rank-only, and the Task-cond. Within RL-only training, replacing the hard threshold with the Gaussian reward brings a modest but consistent improvement on IQA (71.3/71.2 vs. 70.9/71.0), while slightly reducing IAA performance (44.5/45.5 vs. 45.0/45.7). Using Rank-only improves over Gauss.-only on both

tasks, reaching 45.6/45.5 on IAA and 71.7/71.7 on IQA, suggesting that ranking supervision is already an effective signal even without explicit score regression. Using the task-conditioned reward (Task-cond.), which applies Gaussian score reward to IQA and ranking reward to IAA, further improves RL-only performance to 46.0/45.9 on IAA and 72.2/72.1 on IQA, indicating that the two reward forms are complementary when matched to the corresponding task. Under the SFT+RL setting, the reward differences become more pronounced. Hard-only reaches 47.2/44.9 on IAA and 72.2/71.8 on IQA. Switching to Gauss.-only improves both tasks substantially, reaching 49.7/50.7 on IAA and 75.0/74.7 on IQA, corresponding to gains of +2.5/+5.8 and +2.8/+2.9, respectively. Rank-only further outperforms Gauss.-only, achieving 50.3/51.6 on IAA and 75.4/75.6 on IQA, showing that relative ranking becomes especially effective once the model is initialized by SFT. Finally, Task-cond. achieves the best overall results, reaching 51.0/52.5 on IAA and 76.7/76.5 on IQA, improving over Gauss.-only by +1.3/+1.8 on IAA and +1.7/+1.8 on IQA. This confirms that task-matched reward design provides the most effective optimization signal in the two-stage setting.

4.4 Training Dynamics Analysis

Effect of two-stage training. Fig. 6a shows that under RL-only training, IQA completion lengths collapse rapidly toward near-zero within the first ~500 steps, while IAA completions fluctuate without converging. This collapse is the direct behavioral consequence of the reasoning mismatch: without a prior that distinguishes fast and slow response modes, RL uniformly minimizes completion cost. Two-stage training maintains substantially longer and more stable completions for both tasks throughout all 2,000 training steps, with IAA completions remaining noticeably longer than IQA completions as intended. Fig. 6b reinforces this picture: with two-stage training, the IAA format reward rises to near 1.0 within the first ~200 steps and stays stable, whereas RL-only training settles at a substantially lower plateau of around 0.5–0.6 with high variance throughout. This shows that SFT initialization is necessary not only for preserving reasoning length, but for maintaining structural output validity during the RL phase.

Effect of rank reward. Fig. 6c shows that the rank reward increases steadily from around 0.65 at initialization to above 0.90 at convergence, indicating that the model progressively learns

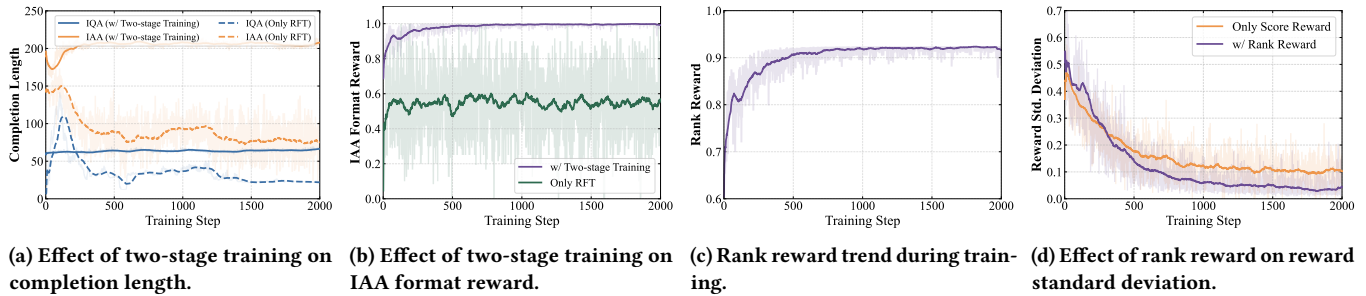


Figure 6: Training dynamics analysis covering completion behavior, reward trends, and optimization stability.

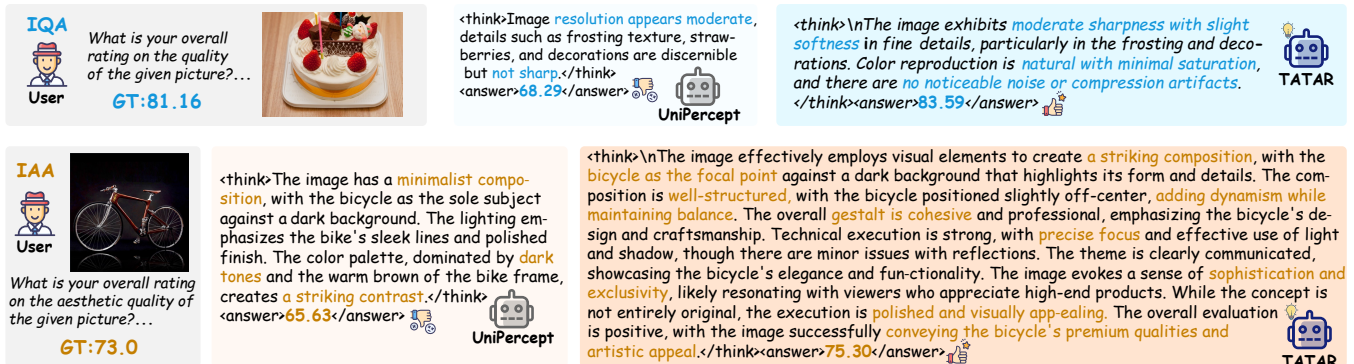


Figure 7: Case study comparing TATAR and UniPercept on representative IQA (top) and IAA (bottom) examples. Ground-truth scores and prediction errors are shown for each model.

stronger relative discrimination among candidate completions. The smooth and monotonic increase suggests that the Thurstone-style pairwise objective provides stable gradients throughout training, without the oscillation often seen in preference-based optimization. Fig. 6d shows that introducing the rank reward reduces the standard deviation of the overall reward by approximately 40–50% compared with score-only training, particularly in the early and mid phases of RL. This reduction in reward variance directly translates to more stable policy updates, confirming that ranking supervision mitigates the reward oscillation that pure score regression introduces on subjective aesthetic data. Together, these dynamics support the core design choice: score-based supervision anchors absolute prediction quality while rank-based supervision stabilizes the relative preference structure that aesthetic assessment requires.

4.5 Case Study

Fig. 7 compares TATAR and UniPercept on representative IQA and IAA examples. On the IQA example, UniPercept produces a coarse judgment based on local discernibility, with a prediction error of 12.87 points. TATAR explicitly identifies sharpness, fine-detail softness, color naturalness, and compression artifacts, reducing the error to 2.43 points. This reflects the fast, distortion-focused reasoning mode instilled by Stage 1 SFT. On the IAA example, the gap is more pronounced. UniPercept relies on three generic visual cues and underestimates the ground truth by 7.37 points. TATAR produces a more integrative assessment covering composition balance,

focal emphasis, craftsmanship, and thematic expression, reducing the error to 2.30 points. This deliberative reasoning reflects the slow IAA mode elicited by our fast–slow construction and asymmetric ranking reward, and is consistent with TATAR’s quantitative gains over UniPercept in Tab. 1.

5 Conclusion

In this work, we revisited unified Image Quality Assessment (IQA) and Image Aesthetic Assessment (IAA) from the perspective of *task-aware reasoning and optimization*. We identified a critical mismatch in prior unified training pipelines: IQA favors concise, distortion-grounded evidence, whereas IAA requires more deliberative, semantics-driven judgment and is poorly served by a uniform regression-style objective. To address this, we propose TATAR, a unified MLLM framework that explicitly separates task-specific *thinking modes and optimization signals*: (i) fast–slow CoT construction for IQA and IAA, (ii) two-stage training with Format SFT followed by GRPO-based RFT, and (iii) asymmetric rewards with Gaussian score shaping for IQA and Thurstone-style completion-level ranking for IAA. Overall, our results suggest that effective unified perceptual scoring requires *task-aware reasoning control* and *reward alignment* rather than a one-size-fits-all objective. In future work, we plan to extend TATAR to broader perceptual tasks (e.g., video quality and aesthetics), explore more faithful and scalable preference supervision, and study continual adaptation under real-world distribution shifts.

References

- [1] Josh Achiam, Steven Adler, Sandhini Agarwal, Lama Ahmad, Ilge Akkaya, Florencia Leoni Aleman, Diogo Almeida, Janko Altenschmidt, Sam Altman, Shyamal Anadkat, et al. 2023. Gpt-4 technical report. *arXiv preprint arXiv:2303.08774* (2023).
- [2] Meta AI. 2025. Llama 4 Scout: A 17B-16E Mixture-of-Experts Multimodal Model. <https://huggingface.co/meta-llama/Llama-4-Scout-17B-16E>. Instruction-tuned MoE model with 10M-token context window.
- [3] Xiang An, Yin Xie, Kaicheng Yang, Wenkang Zhang, Xiuwei Zhao, Zheng Cheng, Yirui Wang, Songcen Xu, Changrui Chen, Didi Zhu, et al. 2025. Llava-onevision-1.5: Fully open framework for democratized multimodal training. *arXiv preprint arXiv:2509.23661* (2025).
- [4] Oron Ansel, Alon Shoshan, Adam Botach, Shunit Haviv Hakimi, Asaf Gendler, Emanuel Ben Baruch, Nadav Bhonker, Igor Kviatkovsky, Manoj Aggarwal, and Gerard Medioni. 2025. Group-Aware Reinforcement Learning for Output Diversity in Large Language Models. *arXiv:2511.12596* [cs.CL] <https://arxiv.org/abs/2511.12596>
- [5] Shuai Bai, Yuxuan Cai, Ruizhe Chen, Keqin Chen, Xionghui Chen, Zesen Cheng, Lianghao Deng, Wei Ding, Chang Gao, Chunjiang Ge, et al. 2025. Qwen3-vl technical report. *arXiv preprint arXiv:2511.21631* (2025).
- [6] Shuai Bai, Keqin Chen, Xuejing Liu, Jialin Wang, Wenbin Ge, Sibao Song, Kai Dang, Peng Wang, Shijie Wang, Jun Tang, Humen Zhong, Yuanzhi Zhu, Mingkun Yang, Zhaohai Li, Jianqiang Wan, Pengfei Wang, Wei Ding, Zheren Fu, Yiheng Xu, Jiabo Ye, Xi Zhang, Tianbao Xie, Zesen Cheng, Hang Zhang, Zhibo Yang, Haiyang Xu, and Junyang Lin. 2025. Qwen2.5-VL Technical Report. *arXiv:2502.13923* [cs.CV] <https://arxiv.org/abs/2502.13923>
- [7] Fatemeh Behrad, Tinne Tuytelaars, and Johan Wagemans. 2025. Charm: the missing piece in vit fine-tuning for image aesthetic assessment. In *Proceedings of the Computer Vision and Pattern Recognition Conference*. 7815–7824.
- [8] Xin Cai, Zhiyuan You, Hailong Zhang, Jinwei Gu, Wentao Liu, and Tianfan Xue. 2024. Phocolors: Photorealistic and consistent reconstruction in lensless imaging. *Advances in Neural Information Processing Systems* 37 (2024), 12219–12242.
- [9] Shuo Cao, Jiayang Li, Xiaohui Li, Yuandong Pu, Kaiwen Zhu, Yuanqing Gao, Siqi Luo, Yi Xin, Qi Qin, Yu Zhou, et al. 2025. UniPercept: Towards Unified Perceptual-Level Image Understanding across Aesthetics, Quality, Structure, and Texture. *arXiv preprint arXiv:2512.21675* (2025).
- [10] Shuo Cao, Nan Ma, Jiayang Li, Xiaohui Li, Lihao Shao, Kaiwen Zhu, Yu Zhou, Yuandong Pu, Jiarui Wu, Jiaquan Wang, et al. 2025. Artimuse: Fine-grained image aesthetics assessment with joint scoring and expert-level understanding. *arXiv preprint arXiv:2507.14533* (2025).
- [11] Du Chen, Tianhe Wu, Kede Ma, and Lei Zhang. 2025. Toward generalized image quality assessment: Relaxing the perfect reference quality assumption. In *Proceedings of the Computer Vision and Pattern Recognition Conference*. 12742–12752.
- [12] Paul F Christiano, Jan Leike, Tom Brown, Miljan Martic, Shane Legg, and Dario Amodei. 2017. Deep reinforcement learning from human preferences. *Advances in neural information processing systems* 30 (2017).
- [13] Yubin Deng, Chen Change Loy, and Xiaoou Tang. 2017. Image aesthetic assessment: An experimental survey. *IEEE Signal Processing Magazine* 34, 4 (2017), 80–106.
- [14] Yuming Fang, Hanwei Zhu, Yan Zeng, Kede Ma, and Zhou Wang. 2020. Perceptual quality assessment of smartphone photography. In *Proceedings of the IEEE/CVF conference on computer vision and pattern recognition*. 3677–3686.
- [15] Junjie Gao, Runze Liu, Yingzhe Peng, Shujian Yang, Jin Zhang, Kai Yang, and Zhiyuan You. 2025. DeQA-Doc: Adapting DeQA-Score to Document Image Quality Assessment. In *Proceedings of the IEEE/CVF International Conference on Computer Vision*. 3428–3437.
- [16] Shuai He, Yongchang Zhang, Rui Xie, Dongxiang Jiang, and Anlong Ming. 2022. Rethinking Image Aesthetics Assessment: Models, Datasets and Benchmarks.. In *IJCAI*, Vol. 6. 22.
- [17] Wenyi Hong, Wenmeng Yu, Xiaotao Gu, Guo Wang, Guobing Gan, Haomiao Tang, Jiale Cheng, Ji Qi, Junhui Ji, Lihang Pan, et al. 2025. Glm-4.5 v and glm-4.1 v-thinking: Towards versatile multimodal reasoning with scalable reinforcement learning. *arXiv preprint arXiv:2507.01006* (2025).
- [18] Vlad Hosu, Hanhe Lin, Tamas Sziranyi, and Dietmar Saupe. 2020. KonIQ-10k: An ecologically valid database for deep learning of blind image quality assessment. *IEEE Transactions on Image Processing* 29 (2020), 4041–4056.
- [19] Gu Jinjin, Cai Haoming, Chen Haoyu, Ye Xiaoxing, Jimmy S Ren, and Dong Chao. 2020. PIPal: a large-scale image quality assessment dataset for perceptual image restoration. In *European conference on computer vision*. Springer, 633–651.
- [20] Chunyi Li, Yuan Tian, Xiaoyue Ling, Zicheng Zhang, Haodong Duan, Haoming Wu, Ziheng Jia, Xiaohong Liu, Xingkuo Min, Guo Lu, et al. 2025. Image quality assessment: From human to machine preference. In *Proceedings of the Computer Vision and Pattern Recognition Conference*. 7570–7581.
- [21] Mingxing Li, Rui Wang, Lei Sun, Yancheng Bai, and Xiangxiang Chu. 2025. Next token is enough: Realistic image quality and aesthetic scoring with multimodal large language model. *arXiv preprint arXiv:2503.06141* (2025).
- [22] Weiqi Li, Xuanyu Zhang, Shijie Zhao, Yabin Zhang, Junlin Li, Li Zhang, and Jian Zhang. 2025. Q-insight: Understanding image quality via visual reinforcement learning. *arXiv preprint arXiv:2503.22679* (2025).
- [23] Zhichao Liao, Xiaokun Liu, Wenyu Qin, Qingyu Li, Qiulin Wang, Pengfei Wan, Di Zhang, Long Zeng, and Pingfa Feng. 2025. Humanaexpert: Advancing a multi-modality foundation model for human image aesthetic assessment. *arXiv preprint arXiv:2503.23907* (2025).
- [24] Hanhe Lin, Vlad Hosu, and Dietmar Saupe. 2019. KADID-10k: A large-scale artificially distorted IQA database. In *2019 Eleventh International Conference on Quality of Multimedia Experience (QoMEX)*. IEEE, 1–3.
- [25] Jack Lindsey, Wes Gurnee, Emmanuel Ameisen, Brian Chen, Adam Pearce, Nicholas L. Turner, Craig Citro, David Abrahams, Shan Carter, Basil Hosmer, Jonathan Marcus, Michael Sklar, Adly Templeton, Trenton Bricken, Callum McDougall, Hoagy Cunningham, Thomas Henighan, Adam Jermy, Andy Jones, Andrew Persic, Zhenyi Qi, T. Ben Thompson, Sam Zimmerman, Kelley Rivoire, Thomas Conerly, Chris Olah, and Joshua Batson. 2025. On the Biology of a Large Language Model. *Transformer Circuits Thread* (2025). <https://transformer-circuits.pub/2025/attribution-graphs/biology.html>
- [26] Dong Liu, Rohit Puri, Nagendra Kamath, and Subhabrata Bhattacharya. 2020. Composition-aware image aesthetics assessment. In *Proceedings of the IEEE/CVF winter conference on applications of computer vision*. 3569–3578.
- [27] Naila Murray, Luca Marchesotti, and Florent Perronnin. 2012. AVA: A large-scale database for aesthetic visual analysis. In *2012 IEEE conference on computer vision and pattern recognition*. IEEE, 2408–2415.
- [28] Long Ouyang, Jeffrey Wu, Xu Jiang, Diogo Almeida, Carroll Wainwright, Pamela Mishkin, Chong Zhang, Sandhini Agarwal, Katarina Slama, Alex Ray, et al. 2022. Training language models to follow instructions with human feedback. *Advances in neural information processing systems* 35 (2022), 27730–27744.
- [29] Daiqing Qi, Handong Zhao, Jing Shi, Simon Jenni, Yifei Fan, Franck Dernoncourt, Scott Cohen, and Sheng Li. 2025. The Photographer’s Eye: Teaching Multimodal Large Language Models to See, and Critique Like Photographers. In *Proceedings of the Computer Vision and Pattern Recognition Conference*. 24807–24816.
- [30] Rafael Rafailov, Archit Sharma, Eric Mitchell, Christopher D Manning, Stefano Ermon, and Chelsea Finn. 2023. Direct preference optimization: Your language model is secretly a reward model. *Advances in neural information processing systems* 36 (2023), 53728–53741.
- [31] Jian Ren, Xiaohui Shen, Zhe Lin, Radomir Mech, and David J Foran. 2017. Personalized image aesthetics. In *Proceedings of the IEEE international conference on computer vision*. 638–647.
- [32] Zhihong Shao, Peiyi Wang, Qihao Zhu, Runxin Xu, Junxiao Song, Xiao Bi, Haowei Zhang, Mingchuan Zhang, YK Li, Yang Wu, et al. 2024. Deepseekmath: Pushing the limits of mathematical reasoning in open language models. *arXiv preprint arXiv:2402.03300* (2024).
- [33] H Sheikh. 2005. LIVE image quality assessment database release 2. <http://live.ece.utexas.edu/research/quality> (2005).
- [34] David Silver, Julian Schrittwieser, Karen Simonyan, Ioannis Antonoglou, Aja Huang, Arthur Guez, Thomas Hubert, Lucas Baker, Matthew Lai, Adrian Bolton, et al. 2017. Mastering the game of go without human knowledge. *nature* 550, 7676 (2017), 354–359.
- [35] Huajie Tan, Yuheng Ji, Xiaoshuai Hao, Xiansheng Chen, Pengwei Wang, Zhongyuan Wang, and Shanghang Zhang. 2025. Reason-rft: Reinforcement fine-tuning for visual reasoning of vision language models. *arXiv preprint arXiv:2503.20752* (2025).
- [36] Gemini Team, Rohan Anil, Sebastian Borgeaud, Jean-Baptiste Alayrac, Jiahui Yu, Radu Soricut, Johan Schalkwyk, Andrew M Dai, Anja Hauth, Katie Millican, et al. 2023. Gemini: a family of highly capable multimodal models. *arXiv preprint arXiv:2312.11805* (2023).
- [37] Daniel Vera Nieto, Luigi Celona, and Clara Fernandez Labrador. 2022. Understanding aesthetics with language: A photo critique dataset for aesthetic assessment. *Advances in Neural Information Processing Systems* 35 (2022), 34148–34161.
- [38] Zhongwei Wan, Zhihao Dou, Che Liu, Yu Zhang, Dongfei Cui, Qinqian Zhao, Hui Shen, Jing Xiong, Yi Xin, Yifan Jiang, et al. 2025. Srpo: Enhancing multimodal llm reasoning via reflection-aware reinforcement learning. *arXiv preprint arXiv:2506.01713* (2025).
- [39] Jiaqi Wang, Kevin Qinghong Lin, James Cheng, and Mike Zheng Shou. 2025. Think or not? selective reasoning via reinforcement learning for vision-language models. *arXiv preprint arXiv:2505.16854* (2025).
- [40] Weiyun Wang, Zhangwei Gao, Lixin Gu, Hengjun Pu, Long Cui, Xingguang Wei, Zhaoyang Liu, Linglin Jing, Shenglong Ye, Jie Shao, et al. 2025. Internvl3. 5: Advancing open-source multimodal models in versatility, reasoning, and efficiency. *arXiv preprint arXiv:2508.18265* (2025).
- [41] Yibin Wang, Zhimin Li, Yuhang Zang, Chunyu Wang, Qinglin Lu, Cheng Jin, and Jiaqi Wang. 2025. Unified multimodal chain-of-thought reward model through reinforcement fine-tuning. *arXiv preprint arXiv:2505.03318* (2025).
- [42] Lai Wei, Yuting Li, Chen Wang, Yue Wang, Linghe Kong, Weiran Huang, and Lichao Sun. 2025. First SFT, Second RL, Third UPT: Continual Improving Multi-Modal LLM Reasoning via Unsupervised Post-Training. *arXiv preprint arXiv:2505.22453* (2025).

- [43] Wen Wen, Tianwu Zhi, Kanglong Fan, Yang Li, Xinge Peng, Yabin Zhang, Yiting Liao, Junlin Li, and Li Zhang. 2025. Self-Evolving Vision-Language Models for Image Quality Assessment via Voting and Ranking. *arXiv preprint arXiv:2509.25787* (2025).
- [44] Haoning Wu, Zicheng Zhang, Weixia Zhang, Chaofeng Chen, Liang Liao, Chunyi Li, Yixuan Gao, Annan Wang, Erli Zhang, Wenxiu Sun, Qiong Yan, Xionghuo Min, Guangtao Zhai, and Weisi Lin. 2024. Q-Align: Teaching LLMs for Visual Scoring via Discrete Text-Defined Levels. In *Proceedings of the 41st International Conference on Machine Learning (Proceedings of Machine Learning Research, Vol. 235)*, Ruslan Salakhutdinov, Zico Kolter, Katherine Heller, Adrian Weller, Nuria Oliver, Jonathan Scarlett, and Felix Berkenkamp (Eds.). PMLR, 54015–54029. <https://proceedings.mlr.press/v235/wu24ah.html>
- [45] Siye Wu, Jian Xie, Yikai Zhang, Aili Chen, Kai Zhang, Yu Su, and Yanghua Xiao. 2025. Arm: Adaptive reasoning model. *arXiv preprint arXiv:2505.20258* (2025).
- [46] Tianhe Wu, Jian Zou, Jie Liang, Lei Zhang, and Kede Ma. 2025. Visualquality-r1: Reasoning-induced image quality assessment via reinforcement learning to rank. *arXiv preprint arXiv:2505.14460* (2025).
- [47] Rui Xie, Anlong Ming, Shuai He, Yi Xiao, and Huadong Ma. 2024. "Special Relativity" of Image Aesthetics Assessment: a Preliminary Empirical Perspective. In *Proceedings of the 32nd ACM International Conference on Multimedia*. 2554–2563.
- [48] Jingyang Yi, Jiazheng Wang, and Sida Li. 2025. ShorterBetter: Guiding Reasoning Models to Find Optimal Inference Length for Efficient Reasoning. [arXiv:2504.21370 \[cs.AI\]](https://arxiv.org/abs/2504.21370) <https://arxiv.org/abs/2504.21370>
- [49] Zhiyuan You, Xin Cai, Jinjin Gu, Tianfan Xue, and Chao Dong. 2025. Teaching large language models to regress accurate image quality scores using score distribution. In *Proceedings of the Computer Vision and Pattern Recognition Conference*. 14483–14494.
- [50] En Yu, Kangheng Lin, Liang Zhao, Jisheng Yin, Yana Wei, Yuang Peng, Haoran Wei, Jianjian Sun, Chunrui Han, Zheng Ge, et al. 2025. Perception-r1: Pioneering perception policy with reinforcement learning. *arXiv preprint arXiv:2504.07954* (2025).
- [51] Shijie Zhao, Xuanyu Zhang, Weiqi Li, Junlin Li, Li Zhang, Tianfan Xue, and Jian Zhang. 2025. Reasoning as Representation: Rethinking Visual Reinforcement Learning in Image Quality Assessment. *arXiv preprint arXiv:2510.11369* (2025).
- [52] Hancheng Zhu, Ju Shi, Zhiwen Shao, Rui Yao, Yong Zhou, Jiaqi Zhao, and Leida Li. 2024. Attribute-driven multimodal hierarchical prompts for image aesthetic quality assessment. In *Proceedings of the 32nd ACM International Conference on Multimedia*. 2399–2408.
- [53] Jie Zhu, Yiyang Su, and Xiaoming Liu. 2026. Can Textual Reasoning Improve the Performance of MLLMs on Fine-grained Visual Classification? *arXiv preprint arXiv:2601.06993* (2026).
- [54] Jinguo Zhu, Weiyun Wang, Zhe Chen, Zhaoyang Liu, Shenglong Ye, Lixin Gu, Hao Tian, Yuchen Duan, Weijie Su, Jie Shao, et al. 2025. Internv13: Exploring advanced training and test-time recipes for open-source multimodal models. *arXiv preprint arXiv:2504.10479* (2025).